

MASSIVE PROTOSTARS IN THE INFRARED DARK CLOUD MSXDC G034.43+00.24

J. M. RATHBORNE, J. M. JACKSON AND E. T. CHAMBERS

Institute for Astrophysical Research, Boston University, Boston, MA 02215; rathborn@bu.edu,
jackson@bu.edu, etc1@bu.edu

R. SIMON

I.Physikalisches Institut, Universität zu Köln, 50937 Köln, Germany; simonr@ph1.uni-koeln.de

AND

R. SHIPMAN AND W. FRIESWIJK

Kapteyn Astronomical Institute, University of Groningen, and Netherlands Institute for Space Research,
P.O. Box 800, 9700 AV Groningen, Netherlands; russ@sron.rug.nl, frieswyk@astro.rug.nl*Draft version October 24, 2018*

ABSTRACT

We present a multiwavelength study of the infrared dark cloud MSXDC G034.43+00.24. Dust emission, traced by millimeter/submillimeter images obtained with the IRAM, JCMT, and CSO telescopes, reveals three compact cores within this infrared dark cloud with masses of 170–800 M_{\odot} and sizes < 0.5 pc. *Spitzer* 3.6–8.0 μm images show slightly extended emission toward these cores, with a spectral enhancement at 4.5 μm that probably arises from shocked H_2 . In addition, the broad line widths ($\Delta V \sim 10 \text{ km s}^{-1}$) of HCN (4–3) and CS (3–2), and the detection of SiO (2–1), observed with the JCMT and IRAM telescopes, also indicate active star formation. *Spitzer* 24 μm images reveal that each of these cores contains a bright, unresolved continuum source; these sources are most likely embedded protostars. Their millimeter to mid-IR continuum spectral energy distributions reveal very high luminosities, 9000–32,000 L_{\odot} . Because such large luminosities cannot arise from low-mass protostars, MSXDC G034.43+00.24 is actively forming massive ($\sim 10 M_{\odot}$) stars.

Subject headings: infrared: stars–ISM: molecules–stars: formation–submillimeter

1. INTRODUCTION

Infrared dark clouds (IRDCs) are a distinct class of interstellar gas cloud discovered in the *Infrared Space Observatory* and *Midcourse Space Experiment* (MSX) Galactic plane mid-IR surveys (Perault et al. 1996; Carey et al. 1998; Hennebelle et al. 2001). IRDCs are identified as dark extinction features seen in silhouette against the bright Galactic background at mid-IR wavelengths. Preliminary studies show that they have high densities ($> 10^5 \text{ cm}^{-3}$), high column densities ($\sim 10^{23} - 10^{25} \text{ cm}^{-2}$), and low temperatures (< 25 K; Egan et al. 1998; Carey et al. 1998, 2000).

It is still unclear what role IRDCs play in star formation. Egan et al. (1998) suggested that IRDCs are quiescent, isolated molecular clumps, not yet actively forming stars. Indeed, if a massive star formed inside an IRDC, it would quickly heat the surrounding natal dust, and thus the IRDC would not remain cold and dark. The detection of compact millimeter and submillimeter (Lis & Carlstrom 1994; Carey et al. 2000; Redman et al. 2003) continuum sources toward some IRDCs, however, suggests that they may harbor prestellar cores. If so, then IRDCs may well play a key role in the very earliest stages of star formation. It is important to determine whether these compact cores are sites of current or future star formation.

In this *Letter*, we use two standard methods to identify sites of active star formation. The first relies on the interaction between a young stellar object (YSO) and its parental molecular cloud. Because YSOs undergo bipolar outflows, they interact strongly with the surrounding

gas and thus can be found by detecting large molecular line widths or shocked gas. One can search for shocks by detecting spectral lines that require shocks for excitation (e.g., H_2) or chemical species that require shocks for their formation (e.g., SiO). The second method relies on the direct detection of the protostar. Because protostars are deeply embedded in dusty clouds, they emit most strongly in the millimeter to IR. Active star-forming cores are thus associated with luminous, highly reddened, compact sources.

We have used both of these methods to discover three distinct sites of active star formation in the IRDC MSXDC G034.43+00.24 (hereafter G34.4+0.2). We identified this IRDC as an extinction feature in the MSX 8 μm Galactic plane survey (Simon et al. 2005). Based on its ^{13}CO emission from the BU-FCRAO Galactic Ring Survey (Simon et al. 2001), we find that G34.4+0.2 is located at a kinematic distance of 3.7 kpc (because it is an IRDC, we assume it lies at the near kinematic distance).

Superposed against this molecular cloud is the compact H II region IRAS 18507+0121 (Bronfman et al. 1996; Molinari et al. 1996). Shepherd et al. (2004) noted a millimeter continuum source (our core MM1) $\sim 40''$ to the north of this H II region. From its weak 6 cm emission, they suggest that this millimeter core contains a deeply embedded B2 protostar. Although Shepherd et al. (2004) did not note that this millimeter core is in fact part of an IRDC, we find that it is indeed embedded within G34.4+0.2. In addition, Garay et al. (2004) detected 1.2 mm continuum emission associated with this cloud in their survey of massive star-forming regions. They note that one core (our

MM3) appears to be a cold (<17 K), massive, dense, and quiescent core.

We find strong evidence to support the idea that these two cores, and one other within G34.4+0.2, are indeed sites of active star formation and will eventually become massive stars ($M \sim 10 M_{\odot}$). The discovery of active massive star formation in this IRDC suggests that IRDCs may be the earliest stage in the formation of high-mass stars.

2. OBSERVATIONS

We present both continuum and spectral line data at many wavelengths (see Table 1 for details). The continuum data cover the wavelength range from 1.2 mm to $24 \mu\text{m}$. The millimeter/submillimeter continuum data were taken at the Institut de Radioastronomie Millimétrique (IRAM), James Clerk Maxwell Telescope (JCMT), and Caltech Submillimeter Observatory (CSO) using either an “on-the-fly” or “scan-mapping” mode. Standard reduction methods within the software packages MOPSIC, CRUSH, and SURF were used to correct for atmospheric opacity and to remove atmospheric fluctuations. The millimeter/submillimeter data were flux-calibrated using either G34.3 or Uranus. The IR continuum data were obtained using the *Spitzer* Space Telescope. The $3.5\text{--}8.0 \mu\text{m}$ images were obtained as part of the Galactic Legacy Infrared Mid-Plane Survey Extraordinaire (GLIMPSE; Benjamin et al. 2003) using the Infrared Array Camera (IRAC). The $24 \mu\text{m}$ images were obtained using the photometry raster mapping mode of the Multi-band Imaging Photometer for *Spitzer* (MIPS). The IRAC data were processed by the GLIMPSE team, and the MIPS data were processed by the *Spitzer* Science Center data processing pipelines.

The spectroscopic data consist of millimeter/submillimeter molecular line observations obtained with IRAM and JCMT. Molecular line spectra toward two of the millimeter cores, MM1 and MM3, within G34.4+0.2 were obtained in SiO (2–1), CS (3–2), HCN (4–3), and C^{18}O (3–2). Chopper wheel calibration, pointing, and focus checks were performed regularly. The data were reduced using standard methods in the software packages GILDAS and SPEX.

3. RESULTS AND DISCUSSION

3.1. Identifying Candidate Protostellar Cores

To locate potential sites of star formation, we have imaged G34.4+0.2 in the millimeter/submillimeter continuum. Because these wavelengths probe cold dust emission, millimeter/submillimeter continuum emission can locate dense compact cores, potential sites of star formation. Our millimeter/submillimeter images of G34.4+0.2 reveal extended, diffuse continuum dust emission that matches the morphology of the mid-IR extinction extremely well. In addition to this extended emission, we also find four compact cores. Figure 1 shows the 1.2 millimeter continuum emission overlaid on a *Spitzer* three-color image ($3.6 \mu\text{m}$ in blue, $4.5 \mu\text{m}$ in green, and $8.0 \mu\text{m}$ in red). One of these cores (MM2) is clearly associated with the H II region IRAS 18507+0121. The remaining three dust cores (MM1, MM3, and MM4) are unresolved (< 0.5 pc) and have 1.2 mm peak fluxes that range from 0.3 to 2.5 Jy beam^{-1} . Table 2 lists their coordinates and peak fluxes.

Because the 1.2 mm continuum emission is optically thin, we can reliably estimate masses via the expression $M = F_{\nu} D^2 / [\kappa_{\nu} B_{\nu}(T)]$, where F_{ν} is the observed flux density, D is the distance, κ_{ν} is the dust opacity per gram of dust, and $B_{\nu}(T)$ is the Planck function at the dust temperature. We adopt for $\kappa_{1.2\text{mm}}$ a value of $1.0 \text{ cm}^2 \text{ g}^{-1}$ (Ossenkopf & Henning 1994). Integrating the 1.2 mm continuum emission above a 3σ level, and assuming a dust temperature of $T_D = 30$ K and a gas-to-dust mass ratio of 100, we find that the total mass of the IRDC is $\sim 7500 M_{\odot}$. Gaussian fits to the three cores reveal masses in the range $170\text{--}800 M_{\odot}$ (see Table 2). The core masses and sizes are similar to massive protostars seen toward other star-forming regions (Brand et al. 2001).

3.2. Evidence of Outflows and Shocked Gas

Evidence of kinematic interactions between embedded YSOs and the molecular gas in these cores can be found in the *Spitzer*/IRAC data. The IRAC three-color 3.5 , 4.6 , and $8.0 \mu\text{m}$ image of G34.4+0.2 reveals slightly extended emission toward all three millimeter cores, with a relative enhancement at $4.5 \mu\text{m}$ (displayed as green). Although highly extinguished stars can appear green in these three color images due to the flat extinction curve between 4.5 and $8.0 \mu\text{m}$ (Indebetouw et al. 2005), bright, extended $4.5 \mu\text{m}$ emission has been found to trace shocked gas in star-forming regions (Marston et al. 2004; Noriega-Crespo et al. 2004). This enhanced $4.5 \mu\text{m}$ emission is thought to arise from shock-excited spectral lines, probably the $\text{H}_2 S(9)$ line at $4.694 \mu\text{m}$. Because these cores show evidence of shocked gas, they are probably forming stars.

Further evidence comes from our IRAM and JCMT molecular line spectra toward two of these cores (Fig. 2). The high-density tracing molecular lines, CS (3–2) and HCN (4–3), show broad line widths ($\Delta V \sim 10 \text{ km s}^{-1}$). Such broad line widths are often interpreted as tracing protostellar outflows (Moriarty-Schieven et al. 1995). Because SiO is thought to form as the result of the shock destruction of dust grains, the SiO (2–1) line indicates strong shocks and is therefore a reliable indicator of star formation (Bachiller et al. 1991; Martin-Pintado et al. 1992; Zhang et al. 1995; Gibb et al. 2004). The strong SiO line, combined with broad lines of the molecular high-density tracers, provides further evidence that active star formation is occurring within these cores.

3.3. Embedded Protostars

A more direct indicator of active star formation is the detection of embedded protostars via their millimeter to IR continuum emission. We have detected embedded protostars toward the three cores using new *Spitzer* $24 \mu\text{m}$ data. The $24 \mu\text{m}$ image of G34.4+0.2 shows that, while the IRDC itself remains dark, the active cores each contain unresolved ($< 6''$), bright $24 \mu\text{m}$ continuum sources (Fig. 1).

We can determine the luminosity of the embedded protostars from their millimeter to IR broadband spectral energy distributions (SEDs). Using the peak fluxes from all of our continuum data in the mid-IR ($24 \mu\text{m}$), submillimeter (350 , 450 , and $850 \mu\text{m}$), and millimeter (1.2 mm), we can construct broadband SEDs and fit them to standard graybody curves (Fig. 3). For simplicity, we assume

that the cores are isothermal. In our fits, the emissivity index (β), optical depth at $250\ \mu\text{m}$ (τ_{250}), and dust temperature (T_D) are free parameters. For a source size of $15''$, these fits yield reasonable values for these parameters: $\beta \sim 1.8$, $\tau_{250} \sim 0.25$, and $T_D \sim 33\ \text{K}$ (see Table 2). The SEDs also provide good estimates for the bolometric luminosity, which is simply the integral under the SED fit. Because these sources are slightly resolved, fits to the SEDs using the peak fluxes will yield lower limits to the actual luminosity. We find that the three protostellar cores in G34.4+0.2 have bolometric luminosities (L_{bol}) of 9000–32,000 L_\odot .

3.4. Large Luminosities: High-Mass Protostars

Theoretical studies of protostellar evolution suggest that low-mass stars ($M < 2 M_\odot$) never achieve luminosities $> 100 L_\odot$ in their pre-main-sequence evolution (Iben 1965). High-mass protostars ($M > 8 M_\odot$), however, evolve at essentially constant luminosity on their path from protostar to main-sequence star (Iben 1965; Palla & Stahler 1990). Thus, the protostellar luminosity is a good indicator of the eventual main-sequence luminosity and, hence, stellar mass. Protostellar luminosities of $\sim 10,000 L_\odot$, therefore, correspond to early B stars with masses of $\sim 10 M_\odot$ (Panagia 1973). Because G34.4+0.2 contains three sites of active star formation with $L_{bol} \sim 10,000 L_\odot$ or more, we conclude that each of these sites contains a massive protostar. Specifically, we find corresponding spectral types of O9.5 for MM1 and B0.5 for both MM3 and MM4 (Panagia 1973).

3.5. The Role of IRDCs in Star Formation

The discovery of active massive star formation in G34.4+0.2 shows that the earliest stages of massive star formation may well take place in IRDCs. Because low-mass stars form within Bok globules, high-mass stars probably form within a higher mass equivalent. We speculate that IRDC cores are indeed these high-mass counterparts to Bok globules. If IRDCs host the earliest stages of high-mass star formation, and then at some point they will spawn OB stars and grow warm. Indeed, the masses and sizes of IRDCs ($M \sim 1000 M_\odot$, sizes approximately a few parsecs) are similar to those of warm molecular clumps associated with massive star-forming regions (Garay & Lizano 1999; Lada & Lada 2003). Moreover, such warm clumps often produce multiple massive stars. The fact that G34.4+0.2 is forming three massive stars and has already formed a B0.5 star associated with the H II region IRAS

18507+0121 (Shepherd et al. 2004) suggests that IRDCs can also form several massive stars almost simultaneously. To test this hypothesis, we are currently searching for more examples of active star formation within a larger sample of IRDCs.

4. CONCLUSIONS

In order to search for regions of active star formation in IRDCs, we have performed a multiwavelength study of the IRDC G34.4+0.2. We identified three potential star-forming cores by finding compact millimeter/submillimeter continuum sources. These cores show enhanced $4.5\ \mu\text{m}$ emission, which is thought to trace shocked gas in star-forming regions. Broad molecular line widths of CS and HCN provide additional evidence of star formation toward two cores. Each of these cores also has strong, broad lines of SiO, a species that preferentially forms in shocks.

We have also directly detected bright, highly reddened, compact sources, presumably protostars, in all three cores. The broadband SEDs of these cores, from millimeter to mid-IR wavelengths, combined with the known kinematic distance, provide a good estimate of their bolometric luminosities, 9000–32,000 L_\odot . Both theoretical and empirical studies suggest that such large luminosities can only arise from high-mass protostars. Hence, G34.4+0.2 contains three active sites of star formation, which will eventually produce massive stars with $M \sim 10 M_\odot$. This study suggests that IRDCs play an important role in the early stages of massive star formation.

The authors gratefully acknowledge funding support through NASA grant NNG04GGC92G. This work is based in part on observations made with the *Spitzer Space Telescope*, which is operated by the Jet Propulsion Laboratory, California Institute of Technology under NASA contract 1407. Support for this work was provided by NASA through contract 1267945 issued by JPL/Caltech. The JCMT is operated by JAC, Hilo, on behalf of the parent organizations of the Particle Physics and Astronomy Research Council in the UK, the National Research Council in Canada, and the Scientific Research Organization of the Netherlands. IRAM is supported by INSU/CNRS (France), MPG (Germany), and IGN (Spain). The CSO telescope is operated by Caltech under a contract from the National Science Foundation (NSF). We would like to thank the GLIMPSE team (PI: E. Churchwell) for providing the IRAC images.

REFERENCES

- Bachiller, R., Martin-Pintado, J., & Fuente, A. 1991, *A&A*, 243, L21
 Benjamin, R. A., et al. 2003, *PASP*, 115, 953
 Brand, J., Cesaroni, R., Palla, F., & Molinari, S. 2001, *A&A*, 370, 230
 Bronfman, L., Nyman, L.-A., & May, J. 1996, *A&AS*, 115, 81
 Carey, S. J., Clark, F. O., Egan, M. P., Price, S. D., Shipman, R. F., & Kuchar, T. A. 1998, *ApJ*, 508, 721
 Carey, S. J., Feldman, P. A., Redman, R. O., Egan, M. P., MacLeod, J. M., & Price, S. D. 2000, *ApJ*, 543, L157
 Egan, M. P., Shipman, R. F., Price, S. D., Carey, S. J., Clark, F. O., & Cohen, M. 1998, *ApJ*, 494, L199
 Garay, G., Faúndez, S., Mardones, D., Bronfman, L., Chini, R., & Nyman, L. 2004, *ApJ*, 610, 313
 Garay, G. & Lizano, S. 1999, *PASP*, 111, 1049
 Gibb, A. G., Richer, J. S., Chandler, C. J., & Davis, C. J. 2004, *ApJ*, 603, 198
 Hennebelle, P., Pérouault, M., Teyssier, D., & Ganesh, S. 2001, *A&A*, 365, 598
 Iben, I. J. 1965, *ApJ*, 141, 993
 Indebetouw, R., et al. 2005, *ApJ*, 619, 931
 Lada, C. J. & Lada, E. A. 2003, *ARA&A*, 41, 57
 Lis, D. C. & Carlstrom, J. E. 1994, *ApJ*, 424, 189
 Marston, A. P., et al. K. 2004, *ApJS*, 154, 333
 Martin-Pintado, J., Bachiller, R., & Fuente, A. 1992, *A&A*, 254, 315
 Molinari, S., Brand, J., Cesaroni, R., & Palla, F. 1996, *A&A*, 308, 573
 Moriarty-Schieven, G. H., Wannier, P. G., Mangum, J. G., Tamura, M., & Olmsted, V. K. 1995, *ApJ*, 455, 190

- Noriega-Crespo, et al. 2004, ApJS, 154, 352
 Ossenkopf, V., & Henning, T. 1994, A&A, 291, 943
 Palla, F. & Stahler, S. W. 1990, ApJ, 360, L47
 Panagia, N. 1973, ApJ, 78, 929
 Perault, M., et al. 1996, A&A, 315, L165
 Redman, R. O., Feldman, P. A., Wyrowski, F., Côté, S., Carey, S. J., & Egan, M. P. 2003, ApJ, 586, 1127
 Shepherd, D. S., Nürnberger, D. E. A., & Bronfman, L. 2004, ApJ, 602, 850
 Simon, R., Jackson, J. M., Clemens, D. P., Bania, T. M., & Heyer, M. H. 2001, ApJ, 551, 747
 Simon, R., Jackson, J. M., Rathborne, J. M., & Chambers, E. T. 2005, ApJ, submitted
 Zhang, Q., Ho, P. T. P., Wright, M. C. H., & Wilner, D. J. 1995, ApJ, 451, L71

TABLE 1
 SUMMARY OF OBSERVATIONS

Telescope	Instrument	Wavelength/ Spectral line	Date	Angular Resolution (")	1σ rms noise
IRAM 30 m	MAMBO-II	1.2 mm	2004 Feb	11	10 mJy
JCMT 15 m	SCUBA	850, 450 μ m	2004 Sept	15, 8	100, 300 mJy
CSO 10 m <i>Spitzer</i>	SHARC-2	350 μ m	2005 Apr	8	500 mJy
	MIPS	24 μ m	2004 Oct	6	70 μ Jy
	IRAC	3.6, 4.5, 8.0 μ m	2003–2004	2	23, 27, 78 μ Jy
IRAM 30 m	C150 Rx	CS (3–2)	2004 Nov	26 ^a	0.13 K
	A100 Rx	SiO (2–1)	2004 Nov	28	0.06 K
JCMT 15 m	B3 Rx	HCN (4–3), C ¹⁸ O (3–2)	2004 Apr	14	0.07, 0.13 K

^aMapped and then smoothed to this resolution

TABLE 2
PARAMETERS FOR THE 1.2 MM CORES WITHIN G34.4+0.2.

Source ^a	Coordinates		Peak Flux					SED fit parameters				
	α (J2000)	δ (J2000)	1.2mm (Jy)	850 μ m (Jy)	450 μ m (Jy)	350 μ m (Jy)	24 μ m (Jy)	$M_{1.2mm}$ ^b (M_{\odot})	β	τ_{250}	T_D (K)	L_{bol} (L_{\odot})
MM1	18 53 18.0	01 25 24	2.5	6.6	70	140	>0.09	800	1.8	0.53	34	32,000
MM3	18 53 20.4	01 28 23	0.3	1.2	10	20	0.03	200	1.8	0.08	32	9,000
MM4	18 53 19.0	01 24 08	0.6	1.8	15	30	0.04	170	1.8	0.13	32	12,000

^aThe cores are named in order of peak 1.2 mm flux (determined from gaussian fits). IRAS 18507+0121 corresponds to our core MM2.

^bCalculated from a gaussian fit to the 1.2 mm emission associated with the core (excluding the underlying emission from the IRDC).

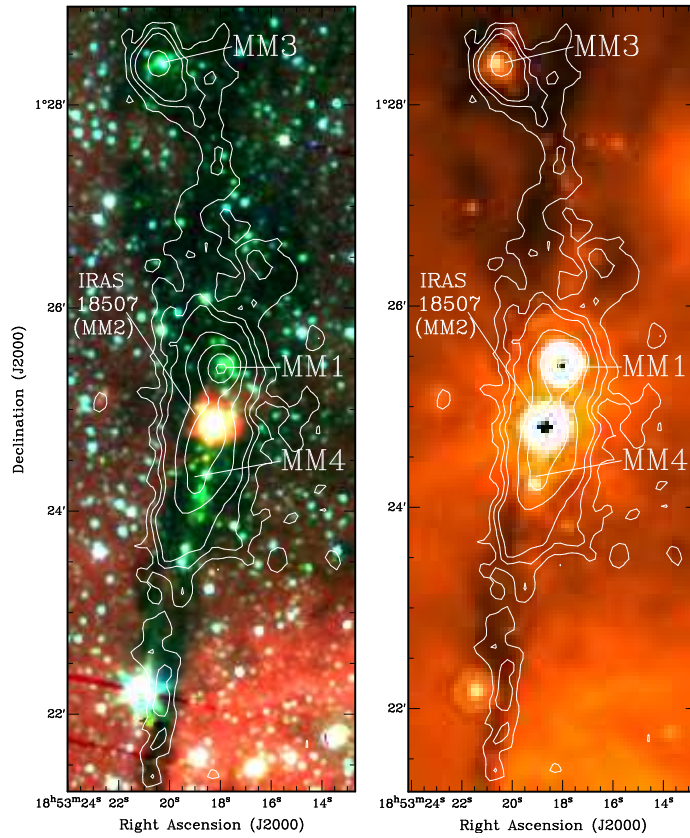


FIG. 1.— G34.4+0.2. *Left:* *Spitzer*/IRAC three-color image (3.6 μ m in blue, 4.5 μ m in green and 8.0 μ m in red) overlaid with IRAM/MAMBO-II 1.2 mm continuum emission (contour levels 60, 90, 120, 240, 480, 1200, and 2200 mJy beam⁻¹). *Right:* *Spitzer*/MIPS 24 μ m image with contours of the IRAM/MAMBO-II 1.2 mm continuum emission (logarithmic color scale, 30 MJy sr⁻¹ [black] to 200 MJy sr⁻¹ [white]). Labeled on this figure are the four millimeter cores.

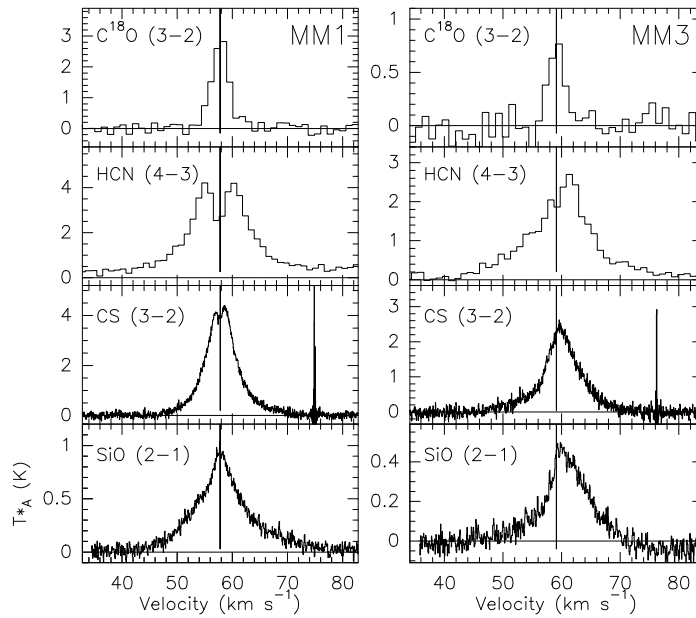


FIG. 2.— IRAM and JCMT molecular line emission toward two of the millimeter cores. The solid vertical line marks the central velocity of the core [as traced by the optically thin $C^{18}O$ (3–2) emission]. Note the broad line widths in the HCN (4–3) and CS (3–2) spectra.

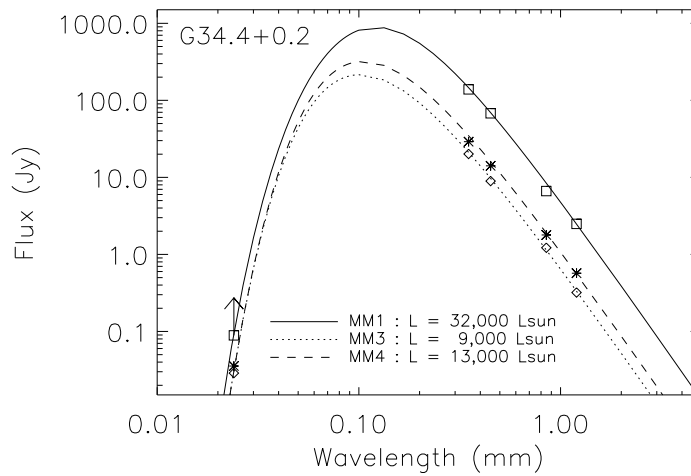


FIG. 3.— Broadband continuum SED for the three cores. Included on this plot are peak fluxes at $24\ \mu\text{m}$, $350\ \mu\text{m}$, $450\ \mu\text{m}$, $850\ \mu\text{m}$, and $1.2\ \text{mm}$. The curves are graybody fits to the data, which yield values of $\beta \sim 1.8$, $\tau_{250} \sim 0.25$, and $T_D \sim 33\ \text{K}$ ($15''$ source diameter; see also Table 2). The derived bolometric luminosities are labeled for each core. MM1 saturates the MIPS array; hence, the quoted $24\ \mu\text{m}$ flux is a lower limit.